Tropical Cyclone Diurnal Cycle as Observed by TRMM

[1]Kenneth D. Leppert II and [2]Daniel J. Cecil
[1]Earth System Science Center
University of Alabama in Huntsville, Huntsville, AL 35899
[2]NASA Marshall Space Flight Center, Huntsville, AL 35805

1. Introduction

▪Using IR satellite data, previous work has shown a consistent diurnal cycle in the pattern of cold cloud tops around tropical cyclones (e.g., Browner et al. 1977; Muramatsu 1983; Lajoie and Butterworth 1984; Steranka et al. 1984; Dunion et al. 2014).

▪Specifically, an increase in the coverage by cold cloud tops often occurs in the inner core of the storm around the time of sunset and subsequently propagates outward to several hundred kilometers over the course of the following day (Dunion et al. 2014).

▪This consistent cycle may have important implications for structure and intensity changes of tropical cyclones and the forecasting of such changes.

▪Goal of this study is to use passive and active microwave measurements from the Tropical Rainfall Measurement Mission (TRMM) Microwave Imager (TMI) and Precipitation Radar (PR), respectively, to better understand the tropical cyclone diurnal cycle throughout a larger depth of the storm's clouds than can be examined using IR satellite measurements alone which are primarily sensitive to cloud top.

2. Method

▪The National Hurricane Center's best track dataset was used to extract all PR and TMI pixels within 1000 km of each tropical cyclone center that occurred in the Atlantic basin between 1998 and 2011.

▪Data was composited according to radius (100-km bins from 0−1000 km) and local standard time (LST; 3-hr bins) for all storms that occurred >300 km from land (Dunion et al. 2014) and had a maximum wind ≥34 kts (i.e., tropical storm or greater intensity).

- PR data was composited by calculating the percentage of pixels with reflectivity ≥20 dBZ at various heights (2−14 km in increments of 2 km).
- Composites of TMI data were created by calculating the percentage of 37.0- and 85.5-GHz polarization corrected temperatures (PCTs; e.g., Toracinta et al. 2002) ≤270 K and ≤260 K, respectively, as a function of radius and time.

▪Composites were created for all storms, as a function of storm intensity, and for storms with 850−200 hPa wind shear ≤15 kts.

▪Several case studies were also examined using passive microwave (TMI, Special Sensor Microwave Imager, and Special Sensor Microwave Imager/Sounder data) and IR (NASA global-merged IR brightness temperature dataset) data.

3. Hurricane Katia (2011)

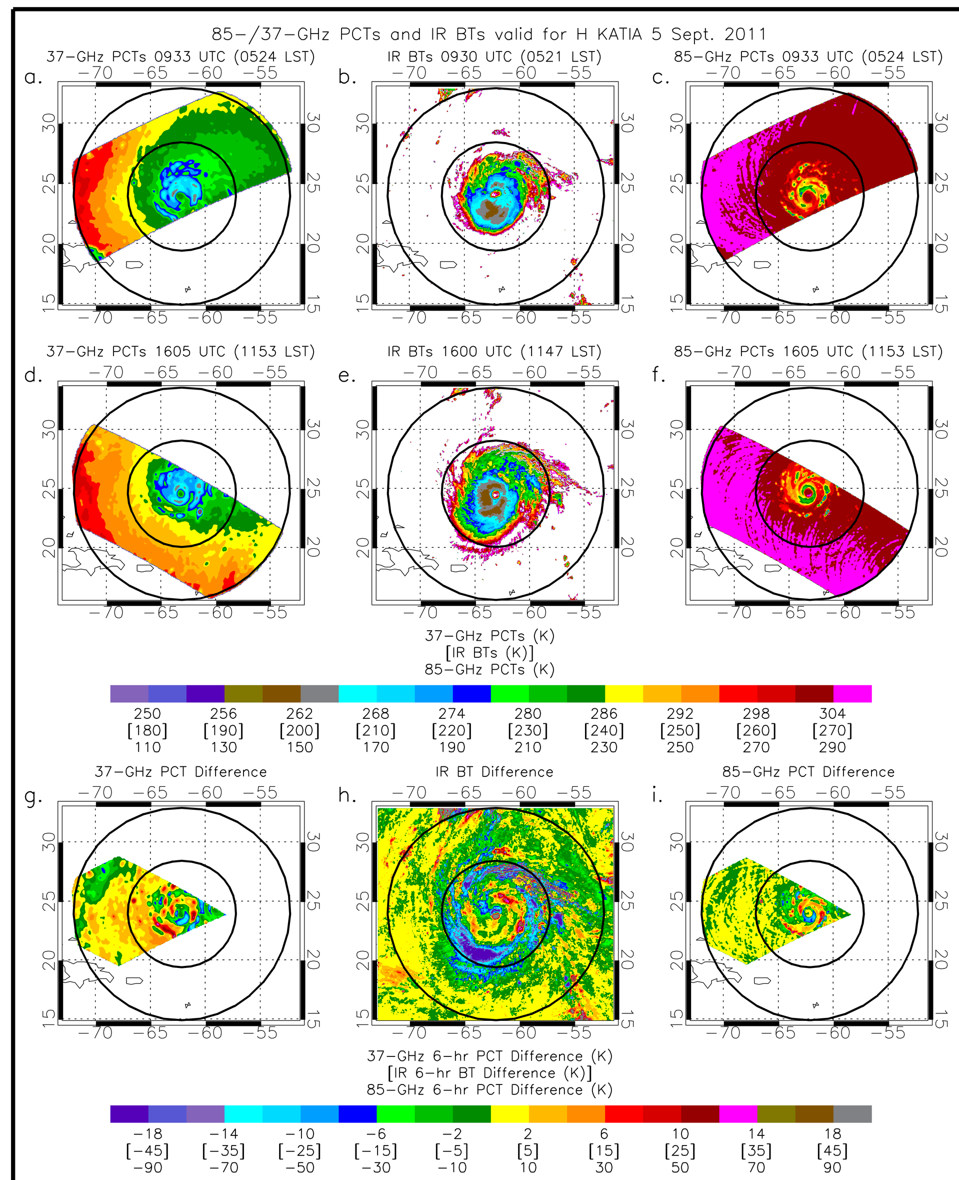

Figure 1. The top row shows a) 37.0-GHz PCTs, b) IR brightness temperatures (BTs), and c) 85.5-GHz PCTs valid at or near 0933 UTC, 5 September 2011 for H. Katia. The second row shows the same as in the first row except valid at or near 1605 UTC, and the third row shows the difference between the first and second rows normalized to 6-hour differences. Note that white areas in b) and e) indicate BTs >275 K, whereas white areas in all other panels indicate missing values. The range rings are for radii of 500 and 1000 km.

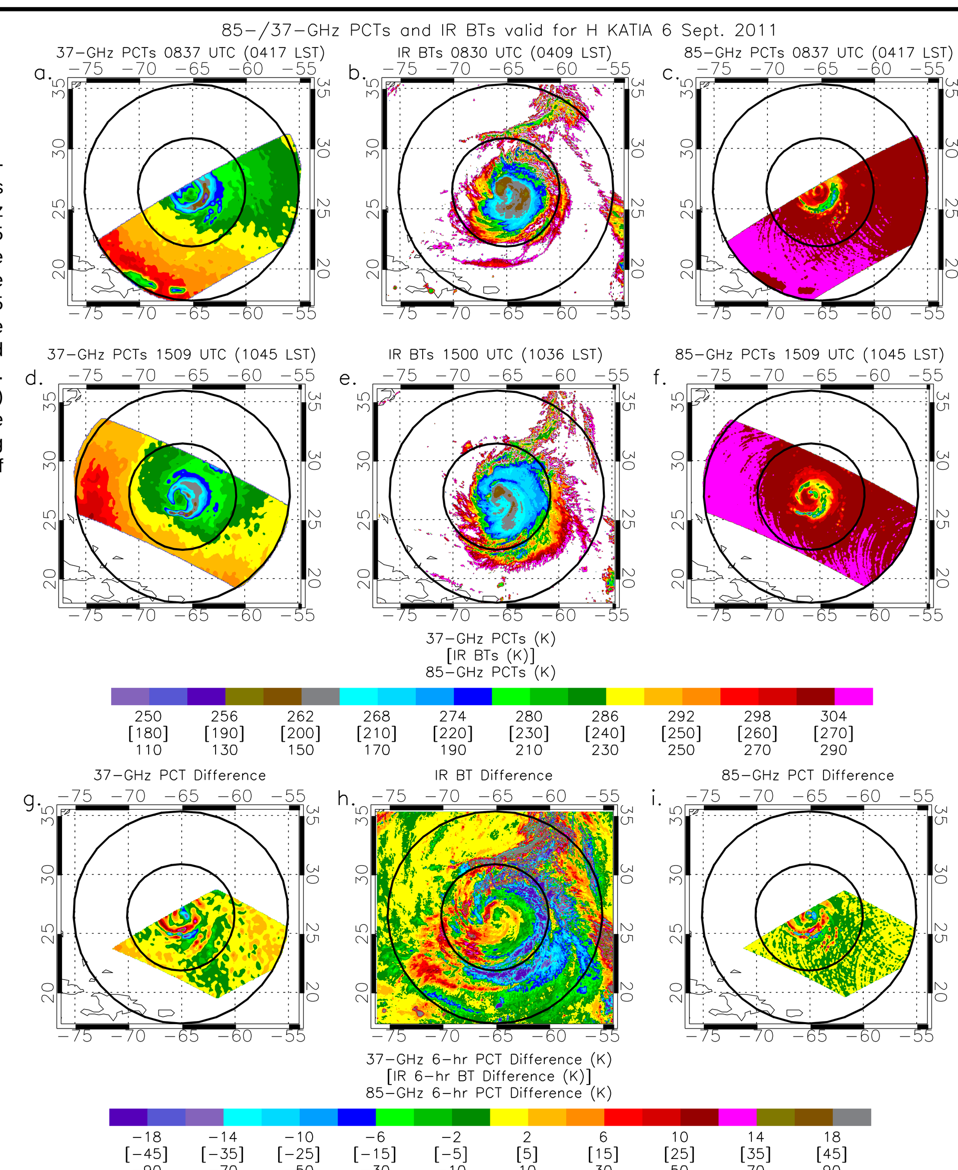

Figure 2. As in Fig. 1, except the top row is valid at or near 0837 UTC, 6 September 2011, and the second row is valid at or near 1509 UTC, 6 September.

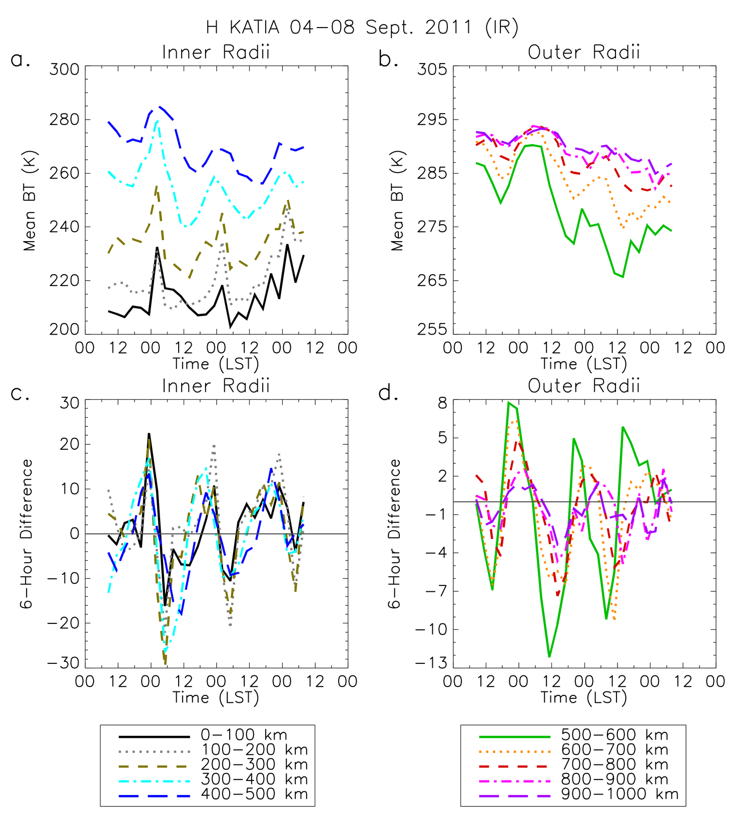

Figure 3. Mean IR BTs for the a) inner radii (<500 km) and b) outer radii (500−1000 km) of H. Katia as a function of LST valid 4–8 September 2011. Corresponding 6-hr BT differences are shown for inner and outer radii in c) and d), respectively.

- Fig. 1 shows an expansion of the IR cold cloud shield with time (panels b and e).
- The IR difference field (Fig. 1h) shows a ring of cooling BTs with time near a radius of 500 km, especially to the south, and a ring of warming BTs just inside this radius indicative of the diurnal pulse described in Dunion et al. (2014).
- The 37- and especially 85-GHz difference fields (Fig. 1g,i) show a similar diurnal pulse feature except at smaller radii than observed in the IR difference field.
- In general, the same features observed in Fig. 1 are observed in Fig. 2, suggesting that these features are consistent from one day to the next.
- The time series of mean IR BTs (6-hr BT differences) shown in Fig. 3 clearly indicate a diurnal cycle for all radii out to ~800 (1000) km.
- In contrast, the corresponding 85.5-GHz times series in Fig. 4 are noisy without any clear indication of a diurnal cycle.

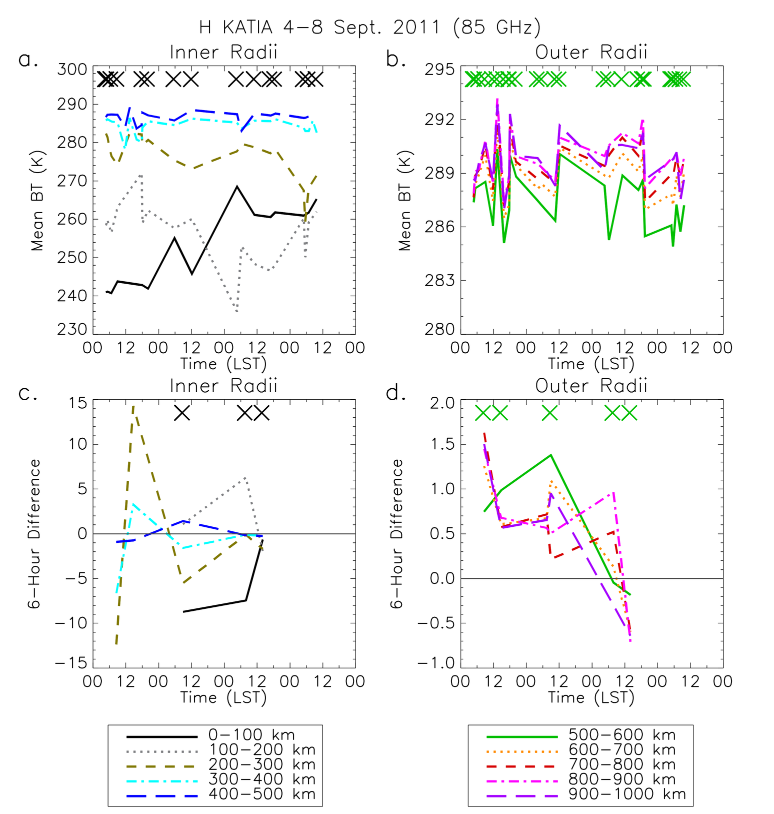

Figure 4. Mean 85.5-GHz PCTs for the a) inner and b) outer radii of H. Katia as a function of LST valid 4–8 September 2011. Corresponding 6-hr PCT differences are shown for inner and outer radii in c) and d), respectively. "X" symbols in each panel indicate times when means or differences were available for the 0–100-km radius in a) and c) and 500–600-km radius in b) and d).

4. PR Composites

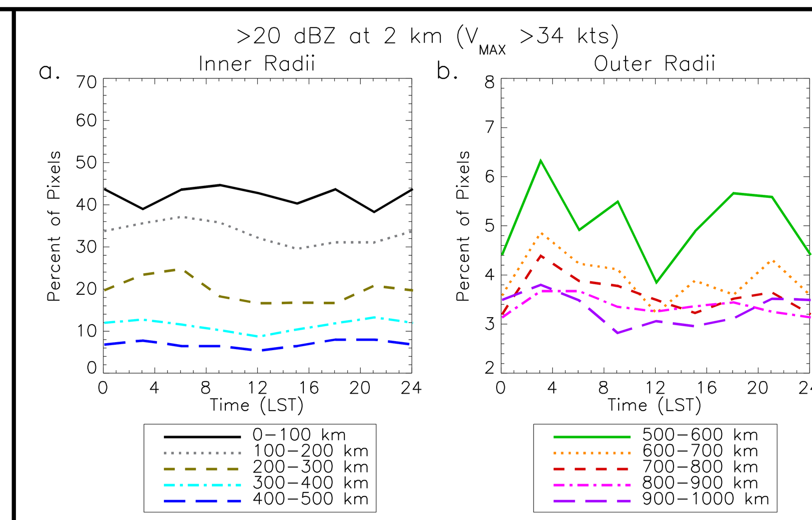

Figure 5. Composite percentage of PR pixels with reflectivity ≥20 dBZ at the 2-km height level for a) inner radii and b) outer radii as a function of LST for all Atlantic tropical cyclones of at least tropical storm strength (i.e., maximum sustained wind [V_{MAX}] ≥34 kts).

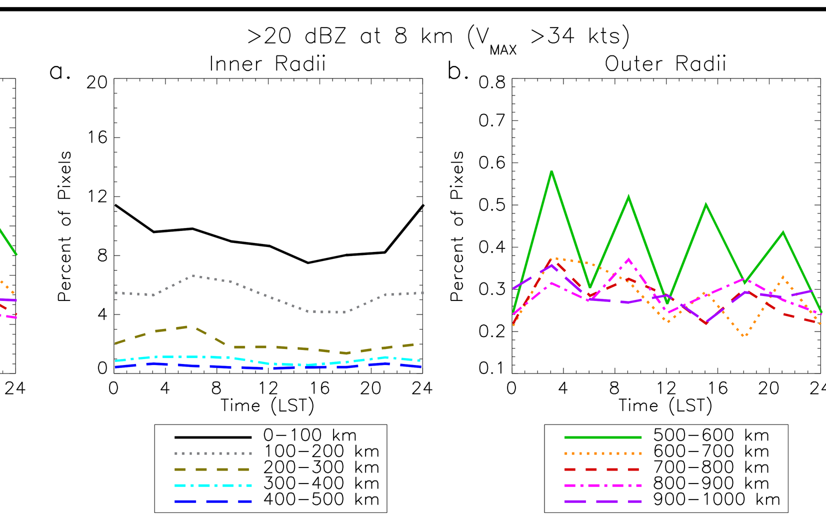

Figure 6. As in Fig. 5, except at a height of 8 km.

- The PR composites using all tropical cyclones with V_{MAX} ≥34 kts suggest a diurnal cycle at radii between 100 and 800 (0 and 300) km at a height of 2 (8) km.
- Some of the radii that suggest a diurnal cycle at the 2-km height level appear to be associated with a double-peaked diurnal cycle or have a single broad peak interrupted by noise.
- There is little indication of the diurnal signal propagating outward with time in these PR composites.

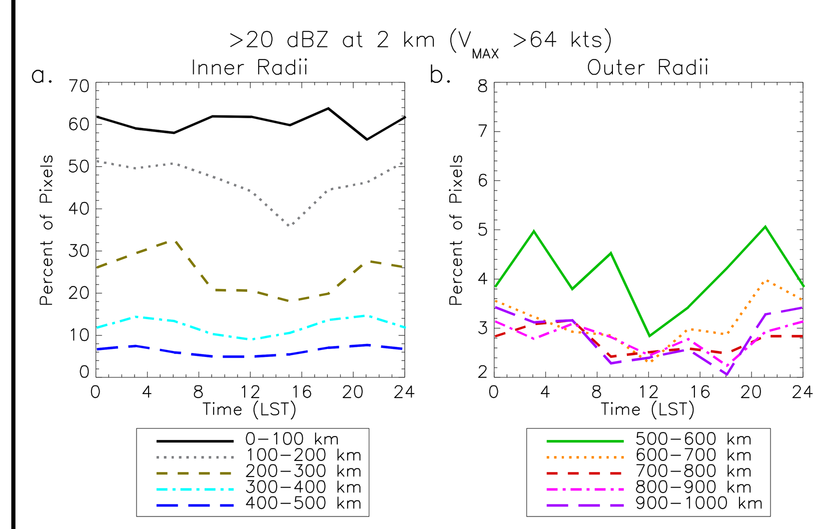

Figure 7. As in Fig. 5, except for Atlantic tropical cyclones of Saffir-Simpson Category 1 strength or higher (i.e., V_{MAX} ≥64 kts)

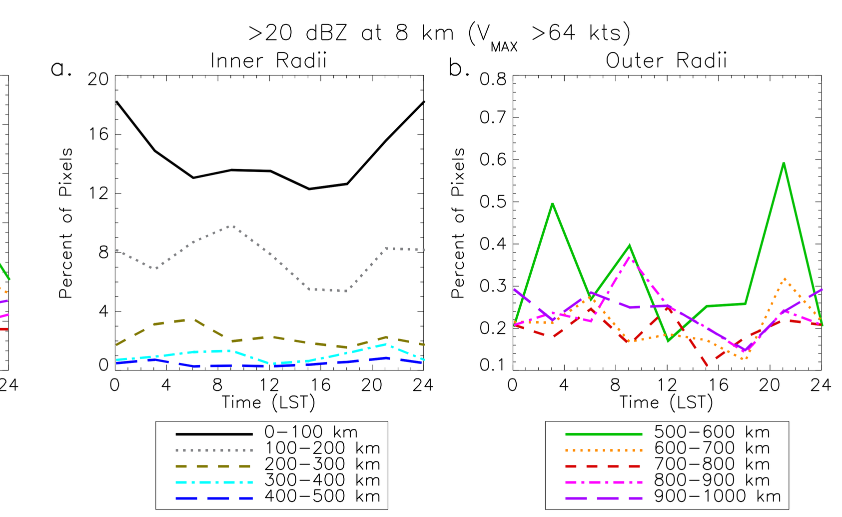

Figure 8. As in Fig. 7, except at a height of 8 km.

- In general, the PR composites using only hurricanes provide similar results to those composites that use tropical storms and hurricanes.
- In particular, at the 2- (8-) km height, the hurricane-only composites suggest a diurnal cycle for radii between 100 and 700 (0 and 400) km.

5. TMI Composites

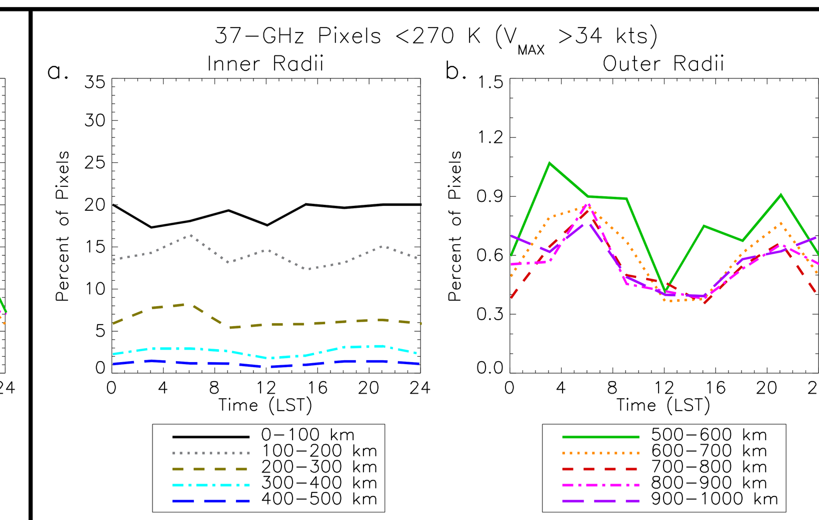

Figure 9. Composite percentage of TMI pixels with 37.0-GHz PCT ≤270 K for a) inner and b) outer radii as a function of LST for all Atlantic tropical cyclones of at least tropical storm strength (i.e., V_{MAX} ≥34 kts).

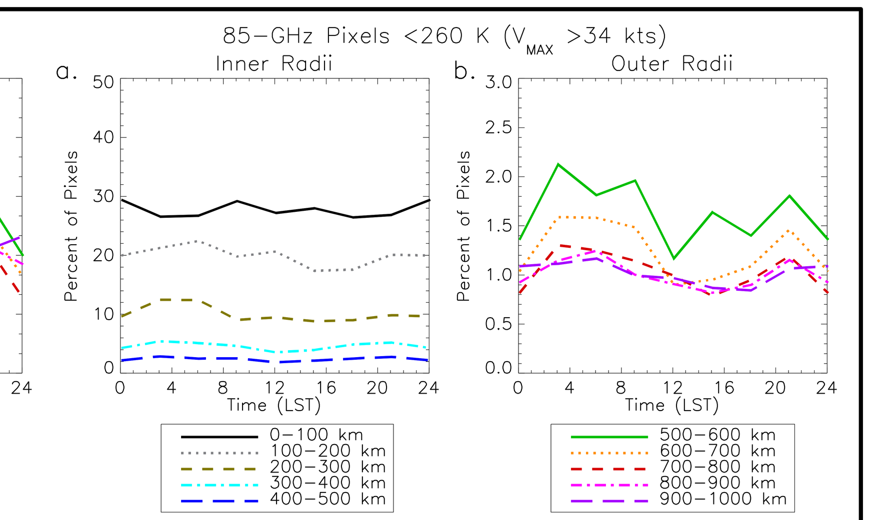

Figure 10. Composite percentage of TMI pixels with 85.5-GHz PCT ≤260 K for a) inner and b) outer radii as a function of LST for all Atlantic tropical cyclones of at least tropical storm strength (i.e., V_{MAX} ≥34 kts).

- The 37.0-GHz TMI composites for all tropical cyclones with V_{MAX} ≥34 kts show patterns that are similar to those seen in the 85.5-GHz composites.
- Specifically, there is little indication of a diurnal cycle for the inner radii (<500 km) at either frequency.
- In contrast, the outer radii (>500 km) of these TMI composites suggest a double-peaked diurnal cycle.

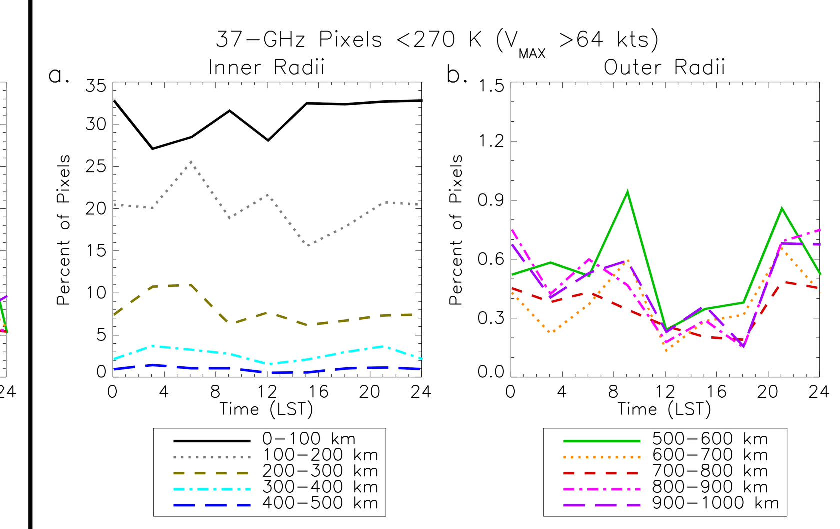

Figure 11. As in Fig. 9, except for Atlantic tropical cyclones of Saffir-Simpson Category 1 strength or higher (i.e., V_{MAX} ≥64 kts).

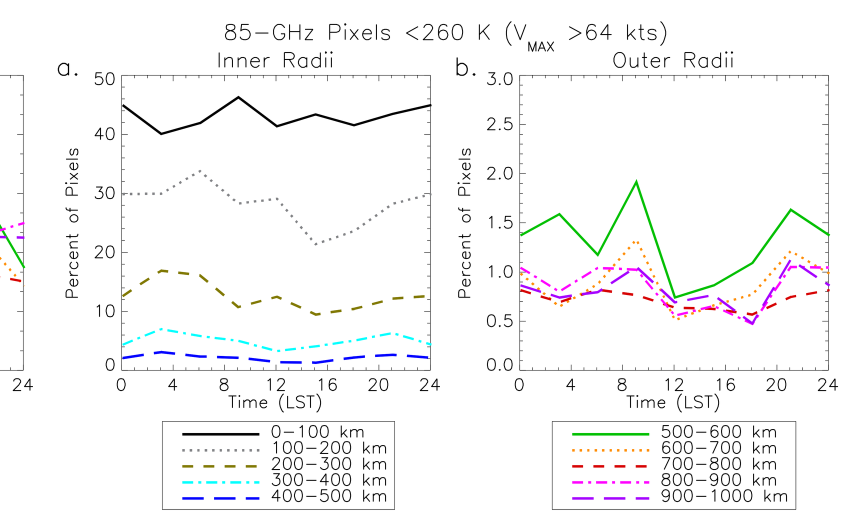

Figure 12. As in Fig. 10, except for Atlantic tropical cyclones of Saffir-Simpson Category 1 strength or higher (i.e., V_{MAX} ≥64 kts).

- Similar to the PR composites, TMI hurricane-only and combined tropical storm / hurricane composites show generally similar patterns (compare Figs. 9 and 11 and Figs. 10 and 12).
- However, the double-peaked diurnal signal observed for outer radii for the combined composites is less clear for the hurricane-only composites, except for the 500–600-km radius.

6. Conclusions

▪The diurnal cycle observed using satellite IR brightness temperatures (BTs) and 6-hour BT differences observed by Dunion et al. (2014) is also generally observed in the cases examined here.

▪No clear diurnal signal is observed for the cases using passive microwave data, but it is not clear whether this is due to irregular sampling and/or calibration differences between sensors or due to storm physics.

▪The PR composites may suggest a diurnal signal at some radii <800 km between a height of 2 and 10 km (some of these radii at lower heights appear to be associated with a double-peaked diurnal signal or perhaps a single broad peak interrupted by noise).

▪Some radii of the 37.0- and 85.5-GHz composites suggest a double-peaked diurnal signal, but, in general, the passive microwave composites provide little evidence of a clear diurnal cycle.

▪Results are not substantially impacted by using storms of different intensity or by removing storms impacted by high wind shear.

Acknowledgement: Funding for this research is generously provided through NASA, grant #NNM11AA01A. We also wish to thank Dr. H. Jiang for her help in identifying TRMM orbits that passed over tropical cyclones.

7. References

▪Browner, S. P., W. L. Woodley, and C. G. Griffith, 1977: Diurnal oscillation of the area of cloudiness associated with tropical storms. *Mon. Wea. Rev.*, **105**, 856−864.

▪Dunion, J. P., C. D. Thorncroft, and C. S. Velden, 2014: The tropical cyclone diurnal cycle of mature hurricanes. *Mon. Wea. Rev.*, **142**, 3900−3919.

▪Lajoie, F. A., and I. J. Butterworth, 1984: Oscillation of high-level cirrus and heavy precipitation around Australian region tropical cyclones. *Mon. Wea. Rev.*, **112**, 535−544.

▪Muramatsu, T., 1983: Diurnal variations of satellite-measured T_{BB} areal distribution and eye diameter of mature typhoons. *J. Meteor. Soc. Japan*, **61**, 77−90.

▪Steranka, J., E. B. Rodgers, and R. C. Gentry, 1984: The diurnal variation of Atlantic Ocean tropical cyclone cloud distribution inferred from geostationary satellite infrared measurements. *Mon. Wea. Rev.*, **112**, 2338−2344.

▪Toracinta, E. R., D. J. Cecil, E. J. Zipser, and S. W. Nesbitt, 2002: Radar, passive microwave, and lightning characteristics of precipitating systems in the tropics. *Mon. Wea. Rev.*, **130**, 802–824.